

Supplementary Materials for

A myocardial infarct border-zone-on-a-chip demonstrates distinct regulation of cardiac tissue function by an oxygen gradient

Megan L. Rexius-Hall *et al.*

Corresponding author: Megan L. McCain, mlmccain@usc.edu

Sci. Adv. **8**, eabn7097 (2022)
DOI: 10.1126/sciadv.abn7097

The PDF file includes:

Supplementary Text
Figs. S1 to S4
Tables S1 to S8
Legends for data S1 to S3

Other Supplementary Material for this manuscript includes the following:

Data S1 to S3

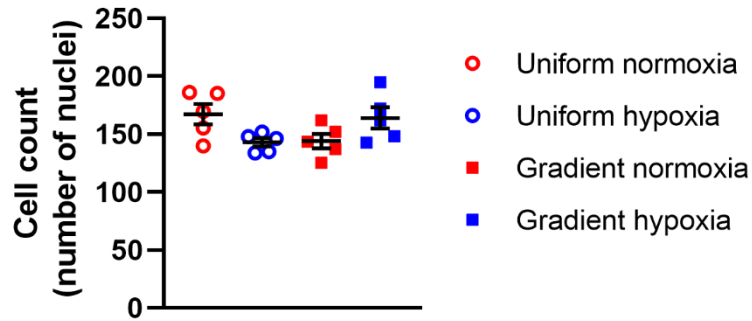


Fig. S1. Cell count as determined from number of nuclei. DAPI staining was used to create a binary mask to count cells in images from the different O₂ conditions. Black lines with error bars indicate mean \pm SEM from n = 5 independent experiments for each condition.

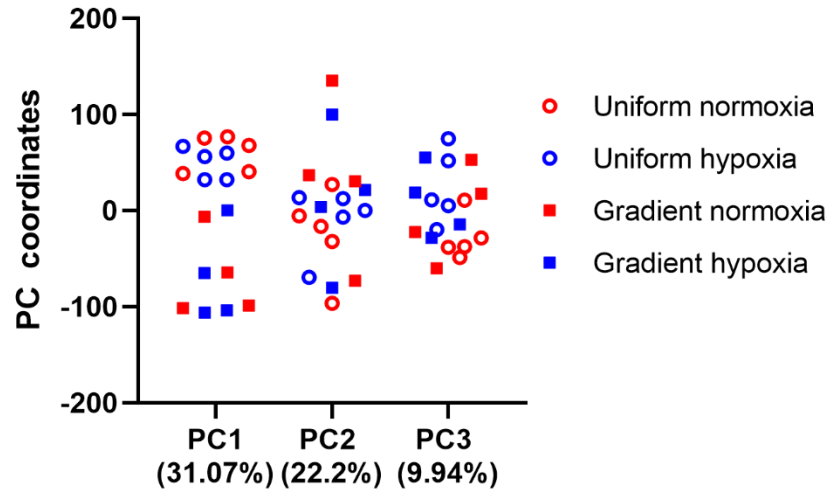


Fig. S2. PC coordinates of the first three principal component axes. PC1 demonstrates clear separation of the gradient from the uniform O₂ conditions.

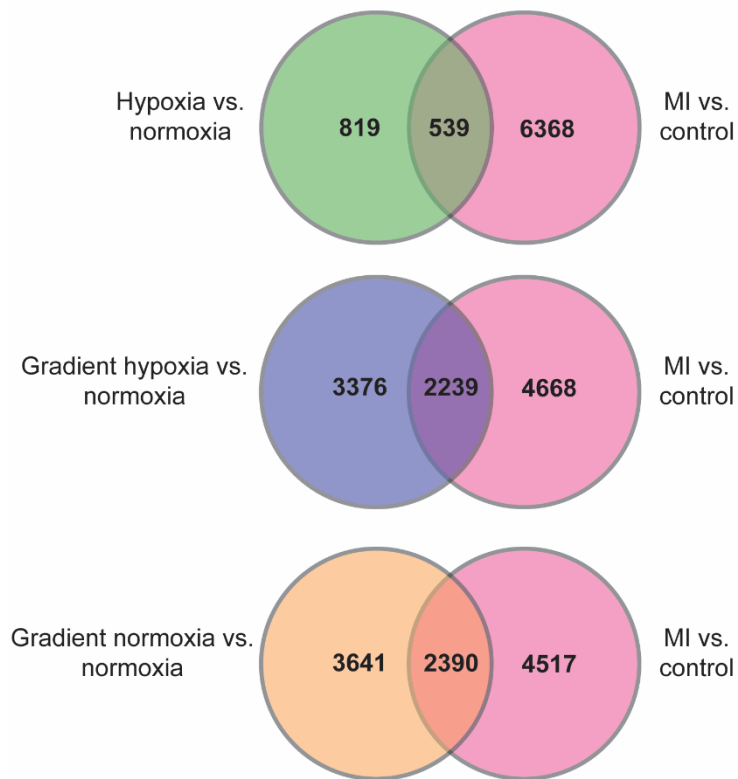


Fig. S3. Venn diagram indicating the overlap of identified DEGs from device conditions and rat MI. Comparison between DEGs ($p < 0.05$) from RNA-seq data of uniform hypoxia or oxygen gradient conditions (versus uniform normoxia) and RNA-seq data from rat 24 h after MI (versus control rat myocardium).

Supplementary Text

Modified Stoney's equation for the two-layer-substrate MTF

Here we derive the modified Stoney's equation for the two-layer-substrate MTF. As shown in Fig. 1, when the cell layer contracts, a tension stress σ_{cell} is generated within the tissue, the thin film is bent into an arc with a radius of curvature R . The modified Stoney's equation is to calculate σ_{cell} from the measured value of R .

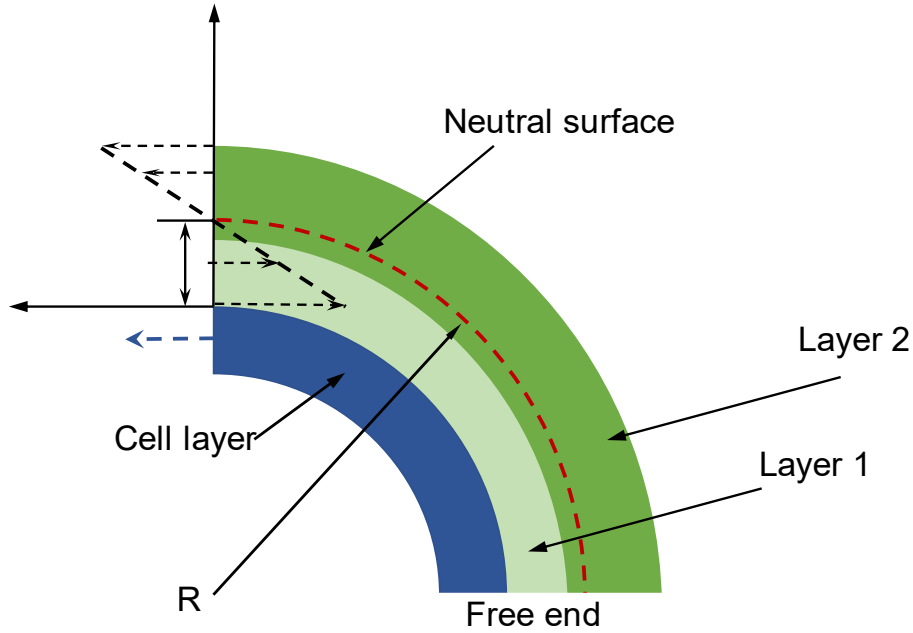


Fig. S4. The free body diagram of a part of the MTF.

Making an imaginary cut to the MTF at a cross section, the part with the free end is selected and the free body diagram is shown in Fig. 1. Note that all the surfaces of this portion of the MTF other than the cut surface are stress-free boundaries. The force and moment equilibrium yields:

$$\int_0^{z_1} \sigma_{x-1}(z) dz + \int_{z_1}^{z_2} \sigma_{x-2}(z) dz + \sigma_{cell} h = 0 \quad (1)$$

$$\int_0^{z_1} z \sigma_{x-1}(z) dz + \int_{z_1}^{z_2} z \sigma_{x-2}(z) dz - \frac{h}{2} \sigma_{cell} h = 0 \quad (2)$$

where σ_{x-i} is the normal stress in the substrate layer i , h is the thickness of the cell layer, $z_1 = t_1$, $z_2 = t_1 + t_2$, t_1 and t_2 are the thickness of the substrate layers (Layer 1 is adjacent to the cell layer). The width of each layer is the same in this work, so it does not appear in Eq. (1) and (2).

For the cylindrical bending of a thin plate, the plain strain assumption is assumed in the width direction, the normal strain $\varepsilon_x(z)$ in the substrate layers can be written as

$$\varepsilon_x(z) = \frac{z - b}{R} \quad (3)$$

where b is the distance between the neutral surface and the cell-substrate interface. By the Hook's law, the normal stress $\sigma_{x-i}(z)$ in the substrate layer i can be written as

$$\sigma_{x-i}(z) = \tilde{E}_i \varepsilon_x(z) \quad (4)$$

where $\tilde{E}_i = \frac{E_i}{(1-\nu_i^2)}$, E_i and ν_i are the Young's modulus and Poisson ratio of the substrate layer i , respectively.

Substituting Eq. (3) and (4) into Eq. (1) and (2), we obtain

$$\frac{\tilde{E}_1}{R} \left(\frac{z_1^2}{2} - bz_1 \right) + \frac{\tilde{E}_2}{R} \left(\frac{z_2^2 - z_1^2}{2} - b(z_2 - z_1) \right) + \sigma_{cell} h = 0 \quad (5)$$

$$\frac{\tilde{E}_1}{R} \left(\frac{z_1^3}{3} - \frac{bz_1^2}{2} \right) + \frac{\tilde{E}_2}{R} \left(\frac{z_2^3 - z_1^3}{3} - \frac{b(z_2^2 - z_1^2)}{2} \right) - \frac{h}{2} \sigma_{cell} h = 0 \quad (6)$$

The two unknowns b and σ_{cell} can be found by solving Eq. (5) and (6):

$$\sigma_{cell} = \frac{2k_1 k_3 - 2k_2^2}{Rh(hk_1 + 2k_2)} \quad (7)$$

$$b = \frac{hk_2 + 2k_3}{hk_1 + 2k_2} \quad (8)$$

where

$$\begin{aligned} k_1 &= \tilde{E}_1 z_1 + \tilde{E}_2 (z_2 - z_1) \\ k_2 &= \frac{\tilde{E}_1 z_1^2}{2} + \frac{\tilde{E}_2 (z_2^2 - z_1^2)}{2} \\ k_3 &= \frac{\tilde{E}_1 z_1^3}{3} + \frac{\tilde{E}_2 (z_2^3 - z_1^3)}{3} \end{aligned}$$

Equation (7) is the modified Stoney's equation for the two-layer-substrate MTF.

Hypoxia vs. Normoxia		Gradient Normoxia vs. Normoxia		Gradient Hypoxia vs. Normoxia		Gradient Hypoxia vs. Hypoxia		Gradient Normoxia vs. Hypoxia	
Gene	FC	Gene	FC	Gene	FC	Gene	FC	Gene	FC
Ankrd37	12.1	Rpph1	60.0	Ereg	44.2	Ereg	55.4	AY172581.2	72.4
Mycl	8.6	AY172581.2	46.8	Cxcl2	40.2	AY172581.2	45.8	Ereg	55.5
Spdef	6.5	Ereg	44.3	AY172581.2	29.6	Tnf	38.3	AABR07029963.1	45.4
Pfkfb3	5.0	Cxcl2	31.5	Tnf	28.2	Rtp3	31.9	AY172581.15	39.8
AABR07049821.2	4.9	AABR07067520.1	30.2	AABR07067520.1	27.9	LOC103694380	31.2	Tnf	33.2
Ddit4	4.8	Slc2a2	24.8	LOC103694380	22.9	Cxcl2	30.8	LOC103694380	28.0
Hk2	4.5	Tnf	24.5	Rtp3	22.8	AABR07029963.1	30.5	AABR07067520.1	27.4
Bhlhe40	4.5	Ripk4	24.1	Ripk4	22.0	Il1a	29.1	Il1a	24.7
Hmox1	4.4	LOC103694380	20.6	Fosb	18.4	AABR07067520.1	25.4	Cxcl2	24.2
Nipal1	4.2	Rtp3	17.0	Evpl	17.0	Bdnf	20.1	Rtp3	23.7
Adm	4.2	Ptgs2	16.9	Ptgs2	15.3	Cxcl10	17.7	Bdnf	21.2
Rgs4	4.1	Fosb	15.8	Bdnf	13.8	Il1b	17.4	Cxcl10	15.8
Ppp1r3b	3.8	Krtap3-2	15.4	Ctrb1	13.8	AY172581.15	15.8	Il1b	15.2
Apold1	3.8	Tbx15	15.2	Il1a	13.7	Adra2a	13.8	Adra2a	15.1
Sik1	3.5	Bdnf	14.6	Cdk5r1	12.7	Ripk4	11.2	Krtap3-2	15.0
Ciart	3.4	Gemin7l1	14.3	Cxcl10	11.8	Evpl	11.0	Ripk4	12.3
Igfals	3.4	LOC100910107	14.3	Adra2a	11.5	Ccl4	10.3	Plk2	11.7
Hunk	2.8	Cxcl1	13.9	Hear2	11.5	Cdk5r1	10.1	Abra	11.4
Glis1	2.7	Ctrb1	13.4	Timm8a2	11.4	Plk2	10.0	LOC100910107	10.8
Trpv1	2.5	Evpl	13.4	Igfals	10.8	Abra	9.9	Pnmt	10.7
Kdm3a	2.5	Cdk5r1	12.7	Tbx15	10.3	Pnmt	9.2	Cdk5r1	10.1
Dtl	2.4	Adra2a	12.6	Krtap3-2	10.3	Clec4e	9.0	Gal3st1	9.5
Errfi1	2.4	AABR07029963.1	12.4	AABR07021465.1	10.0	Serpib2	8.9	AABR07034750.1	9.4
Zfp3612	2.2	Il1a	11.6	Csrp1	9.8	Iqsec3	8.7	Evpl	8.7
LOC100911319	2.2	Ampd1	11.1	Ankrd2	9.6	AABR07021465.1	8.5	Serpib2	8.6
Zfc3h1	-2.1	Aplnr	-8.5	Kenk3	-7.7	Hils1	-7.3	LOC100911101	-8.2
Mycn	-2.1	Zkscan8	-8.7	Tspear	-7.9	Tspear	-7.5	Pabpc4l	-8.2
Lurap1	-2.1	Smim5	-8.9	Bbs10	-7.9	Rrad	-7.5	Drd1	-8.2
Slc35d2	-2.2	Bik	-9.1	Gpr157	-8.0	Nfe2	-7.5	Rrad	-8.5
Zfp2	-2.3	Cpne5	-9.1	Lmo3	-8.0	Pik3c2g	-7.6	Nipal1	-8.7
Purg	-2.3	Lmo3	-9.2	Bik	-8.1	Asb10	-7.6	Pik3ip1	-8.9
Nfkbid	-2.3	Nr0b2	-9.2	Zfp763	-8.1	G0s2	-8.0	Zfp763	-8.9
Klf8	-2.7	LOC100911101	-9.3	AC142138.2	-8.3	Cited4	-8.2	Slc6a7	-9.0
Plcx3	-2.8	Hist2h2be	-9.3	Aplnr	-8.3	Hist2h2be	-8.2	Gpr183	-9.3
Kcna4	-3.0	Sgpp2	-9.4	Zkscan8	-8.4	Pik3ip1	-8.4	Hba-a2	-9.8
Gpr88	-3.5	Palm3	-9.6	Pcare	-8.4	Pcare	-8.5	Gpr34	-9.8
Eppin	-4.2	Cited4	-9.8	Palm3	-8.5	Bmf	-8.8	Edaradd	-11.1
		Gpr34	-9.9	Klhl33	-8.6	Zfp955a	-8.8	Arrdc3	-11.9
		Pabpc4l	-10.0	Nr0b2	-8.7	Ddit4	-9.2	Klhl33	-12.5
		LOC103690139	-10.2	Hba-a1	-8.8	Klhl33	-9.7	Tspear	-12.5
		Efhd1	-10.6	Zfp955a	-8.9	Arrdc3	-9.8	LOC102553613	-12.7
		Klhl33	-11.1	Smim5	-9.5	Zfp763	-11.0	Gpr157	-12.8
		Gask1a	-11.1	Sgpp2	-9.8	AC130146.1	-11.6	Ddit4	-12.9
		Lgr6	-11.9	Cited4	-10.7	LOC102553613	-11.9	Syt6	-13.0
		LOC102553613	-13.1	AC130146.1	-10.7	Palm3	-12.0	Palm3	-13.5
		Tspear	-13.2	Nfe2	-10.9	Gpr157	-12.7	Hist2h2be	-13.9
		Elfn2	-14.4	Gask1a	-11.0	Syt6	-13.4	Hba-a1	-14.2
		AC130146.1	-15.2	LOC102553613	-12.3	Depp1	-14.4	Depp1	-16.4
		Hba-a2	-15.8	Asb10	-13.3	RGD1566386	-16.9	AC130146.1	-16.5
		Hba-a1	-21.5	RGD1566386	-17.8	Gask1a	-19.2	Gask1a	-19.4

Table S1. Differentially expressed gene list. The 25 upregulated and 25 downregulated DEGs with the highest |fold change| (FC) ($p < 0.05$, and $FDR < 0.05$). Note that in the hypoxia vs. normoxia comparison there are only 12 downregulated genes (see Fig. 5G).

Pathway	$-\log(p\text{-value})$
HIF1 α Signaling	7.54
Antioxidant Action of Vitamin C	6.30
G-Protein Coupled Receptor Signaling	5.33
Breast Cancer Regulation by Stathmin1	4.87
CREB Signaling in Neurons	4.22
Renal Cell Carcinoma Signaling	4.20
TNFR1 Signaling	4.10
ERK/MAPK Signaling	4.02
TNFR2 Signaling	3.82
G α i Signaling	3.74
MIF-mediated Glucocorticoid Regulation	3.62
Endothelin-1 Signaling	3.62
Role of MAPK Signaling in Promoting the Pathogenesis of Influenza	3.40
CDK5 Signaling	3.40
Angiotensin Signaling	3.29
MIF Regulation of Innate Immunity	3.28
NF- κ B Activation by Viruses	3.27
Toll-like Receptor Signaling	3.27
VEGF Family Ligand-Receptor Interactions	3.12
cAMP-mediated signaling	3.10
IL-6 Signaling	3.09
Xenobiotic Metabolism Signaling	3.07
Tumor Microenvironment Pathway	3.06
Ceramide Signaling	2.99
CCR3 Signaling in Eosinophils	2.97
STAT3 Pathway	2.97
Acute Phase Response Signaling	2.97
Synaptic Long-Term Depression	2.85
Role of Macrophages, Fibroblasts and Endothelial Cells in Rheumatoid Arthritis	2.71
Phospholipases	2.62
Opioid Signaling Pathway	2.59
Human Embryonic Stem Cell Pluripotency	2.52
IL-10 Signaling	2.48
Hypoxia Signaling in the Cardiovascular System	2.44
Role of MAPK Signaling in Inhibiting the Pathogenesis of Influenza	2.39
Axonal Guidance Signaling	2.38
Synaptic Long-Term Potentiation	2.30
Role of MAPK Signaling in the Pathogenesis of Influenza	2.29
fMLP Signaling in Neutrophils	2.28
April Mediated Signaling	2.26
G α 12/13 Signaling	2.25
PEDF Signaling	2.24
B Cell Activating Factor Signaling	2.24
LPS-stimulated MAPK Signaling	2.22
Sperm Motility	2.21
PPAR α /RXR α Activation	2.20
D-myo-inositol-5-phosphate Metabolism	2.20
BMP signaling pathway	2.19
Insulin Receptor Signaling	2.16
Dermatan Sulfate Biosynthesis (Late Stages)	2.15

Table S2. Pathway analysis of hypoxia vs. normoxia. Top 50 significant pathways ($p < 0.05$) identified from DEGs using Ingenuity Pathway Analysis.

Pathway	-log(p-value)
Systemic Lupus Erythematosus in B Cell Signaling Pathway	7.34
Colorectal Cancer Metastasis Signaling	7.32
Role of Pattern Recognition Receptors in Recognition of Bacteria and Viruses	6.99
Neuroinflammation Signaling Pathway	6.74
HMGB1 Signaling	6.27
G-Protein Coupled Receptor Signaling	6.16
CREB Signaling in Neurons	6.08
Role of Macrophages, Fibroblasts and Endothelial Cells in Rheumatoid Arthritis	5.94
Toll-like Receptor Signaling	5.84
Endothelin-1 Signaling	5.80
CD40 Signaling	5.64
Gαq Signaling	5.62
Axonal Guidance Signaling	5.47
IL-8 Signaling	5.20
IL-17 Signaling	5.14
Breast Cancer Regulation by Stathmin1	4.99
CXCR4 Signaling	4.89
TREM1 Signaling	4.72
Superpathway of Inositol Phosphate Compounds	4.61
IL-10 Signaling	4.55
Fc Epsilon RI Signaling	4.53
Regulation of the Epithelial Mesenchymal Transition by Growth Factors Pathway	4.49
Glioma Invasiveness Signaling	4.47
B Cell Receptor Signaling	4.40
Erythropoietin Signaling Pathway	4.39
IL-6 Signaling	4.35
Cardiac Hypertrophy Signaling	4.33
Cardiac Hypertrophy Signaling (Enhanced)	4.32
Neurotrophin/TRK Signaling	4.23
Apelin Endothelial Signaling Pathway	4.19
FcγRIIB Signaling in B Lymphocytes	4.11
LPS-stimulated MAPK Signaling	4.11
Role of IL-17A in Arthritis	4.05
PDGF Signaling	4.04
ErbB Signaling	4.02
IL-1 Signaling	4.02
Opioid Signaling Pathway	4.01
Semaphorin Neuronal Repulsive Signaling Pathway	4.00
STAT3 Pathway	3.97
Relaxin Signaling	3.91
P2Y Purigenic Receptor Signaling Pathway	3.84
IL-23 Signaling Pathway	3.82
Adrenomedullin Signaling Pathway	3.81
Sperm Motility	3.80
Th1 Pathway	3.78
Production of Nitric Oxide and Reactive Oxygen Species in Macrophages	3.77
Endocannabinoid Developing Neuron Pathway	3.73
GDNF Family Ligand-Receptor Interactions	3.69
Role of Tissue Factor in Cancer	3.66
Role of JAK1 and JAK3 in γc Cytokine Signaling	3.66

Table S3. Pathway analysis of gradient normoxia vs. normoxia. Top 50 significant pathways ($p < 0.05$) identified from DEGs using Ingenuity Pathway Analysis.

Pathway	-log(p-value)
Colorectal Cancer Metastasis Signaling	8.34
Endothelin-1 Signaling	6.28
Glioma Invasiveness Signaling	5.94
Neuroinflammation Signaling Pathway	5.84
Neurotrophin/TRK Signaling	5.67
Axonal Guidance Signaling	5.44
Regulation Of the Epithelial Mesenchymal Transition by Growth Factors Pathway	5.30
IL-8 Signaling	5.29
Superpathway of Inositol Phosphate Compounds	5.17
Cardiac Hypertrophy Signaling	4.96
STAT3 Pathway	4.96
Toll-like Receptor Signaling	4.87
ErbB Signaling	4.87
Role of Macrophages, Fibroblasts and Endothelial Cells in Rheumatoid Arthritis	4.76
Role of IL-17A in Arthritis	4.74
HMGB1 Signaling	4.71
CREB Signaling in Neurons	4.71
Tumor Microenvironment Pathway	4.59
Endocannabinoid Cancer Inhibition Pathway	4.53
Sphingosine-1-phosphate Signaling	4.43
PDGF Signaling	4.29
CXCR4 Signaling	4.27
Apelin Endothelial Signaling Pathway	4.27
Estrogen-Dependent Breast Cancer Signaling	4.21
Adrenomedullin signaling pathway	4.15
Endocannabinoid Developing Neuron Pathway	4.15
Gαq Signaling	4.14
Glioblastoma Multiforme Signaling	4.10
UVA-Induced MAPK Signaling	4.07
JAK/Stat Signaling	4.00
Fc Epsilon RI Signaling	3.99
CD40 Signaling	3.91
IL-4 Signaling	3.91
IL-6 Signaling	3.90
P2Y Purigenic Receptor Signaling Pathway	3.85
FcγRIIB Signaling in B Lymphocytes	3.81
HIF1α Signaling	3.81
ILK Signaling	3.80
Phagosome Formation	3.80
IL-2 Signaling	3.76
Role of Hypercytokinemia/hyperchemokineemia in the Pathogenesis of Influenza	3.75
Thrombin Signaling	3.74
IL-23 Signaling Pathway	3.73
Production of Nitric Oxide and Reactive Oxygen Species in Macrophages	3.69
Breast Cancer Regulation by Stathmin1	3.67
Sperm Motility	3.65
Thyroid Cancer Signaling	3.65
G-Protein Coupled Receptor Signaling	3.63
ERK/MAPK Signaling	3.60
FLT3 Signaling in Hematopoietic Progenitor Cells	3.59

Table S4. Pathway analysis of gradient hypoxia vs. normoxia. Top 50 significant pathways ($p < 0.05$) identified from DEGs using Ingenuity Pathway Analysis.

Pathway	-log(p-value)
Breast Cancer Regulation by Stathmin1	10.90
CREB Signaling in Neurons	10.50
IL-17 Signaling	8.30
Tumor Microenvironment Pathway	7.67
Role of Macrophages, Fibroblasts and Endothelial Cells in Rheumatoid Arthritis	7.37
Role of IL-17A in Arthritis	6.89
G-Protein Coupled Receptor Signaling	6.77
HMGB1 Signaling	6.74
Cardiac Hypertrophy Signaling (Enhanced)	6.65
Colorectal Cancer Metastasis Signaling	6.62
PPAR Signaling	6.56
IL-6 Signaling	6.31
Toll-like Receptor Signaling	5.58
LXR/RXR Activation	5.49
STAT3 Pathway	5.33
Acute Phase Response Signaling	5.30
Hepatic Fibrosis Signaling Pathway	5.30
Granulocyte Adhesion and Diapedesis	5.12
Gαq Signaling	5.05
Superpathway of Inositol Phosphate Compounds	5.05
Production of Nitric Oxide and Reactive Oxygen Species in Macrophages	5.03
IL-1 Signaling	5.03
Role of Osteoblasts, Osteoclasts and Chondrocytes in Rheumatoid Arthritis	4.98
Role of Hypercytokinemia/hyperchemokine in the Pathogenesis of Influenza	4.97
NF-κB Activation by Viruses	4.93
Cardiac Hypertrophy Signaling	4.93
HIF1α Signaling	4.76
MSP-RON Signaling in Macrophages Pathway	4.74
Systemic Lupus Erythematosus in B Cell Signaling Pathway	4.66
Apelin Endothelial Signaling Pathway	4.61
IL-9 Signaling	4.60
Endothelin-1 Signaling	4.59
Th1 and Th2 Activation Pathway	4.50
Differential Reg. of Cytokine Production in Intestinal Epithelial Cells by IL-17A/IL-17F	4.47
Th1 Pathway	4.47
Hepatic Fibrosis / Hepatic Stellate Cell Activation	4.46
Neurotrophin/TRK Signaling	4.45
ErbB Signaling	4.45
Axonal Guidance Signaling	4.32
Human Embryonic Stem Cell Pluripotency	4.31
Erythropoietin Signaling Pathway	4.29
Role of Pattern Recognition Receptors in Recognition of Bacteria and Viruses	4.29
Hepatic Cholestasis	4.24
IL-8 Signaling	4.23
Neuroinflammation Signaling Pathway	4.20
Agranulocyte Adhesion and Diapedesis	4.12
Regulation of the Epithelial Mesenchymal Transition by Growth Factors Pathway	4.12
3-phosphoinositide Biosynthesis	4.12
Acute Myeloid Leukemia Signaling	4.07
JAK/Stat Signaling	4.05

Table S5. Pathway analysis of gradient hypoxia vs. hypoxia. Top 50 significant pathways ($p < 0.05$) identified from DEGs using Ingenuity Pathway Analysis.

Pathway	-log(p-value)
Breast Cancer Regulation by Stathmin1	9.74
CREB Signaling in Neurons	9.74
Axonal Guidance Signaling	9.29
Hepatic Fibrosis Signaling Pathway	8.55
Role of Macrophages, Fibroblasts and Endothelial Cells in Rheumatoid Arthritis	8.17
Cardiac Hypertrophy Signaling (Enhanced)	8.10
G-Protein Coupled Receptor Signaling	7.47
Systemic Lupus Erythematosus in B Cell Signaling Pathway	7.42
Role of Osteoblasts, Osteoclasts and Chondrocytes in Rheumatoid Arthritis	7.42
Colorectal Cancer Metastasis Signaling	7.37
Human Embryonic Stem Cell Pluripotency	6.85
Tumor Microenvironment Pathway	6.08
P2Y Purigenic Receptor Signaling Pathway	5.54
PPAR Signaling	5.39
HMGB1 Signaling	5.32
Fc Epsilon RI Signaling	5.26
NF- κ B Activation by Viruses	5.26
Superpathway of Inositol Phosphate Compounds	5.21
IL-17 Signaling	5.21
ErbB Signaling	5.20
Osteoarthritis Pathway	5.17
G α q Signaling	5.16
Regulation of the Epithelial Mesenchymal Transition by Growth Factors Pathway	4.97
Acute Myeloid Leukemia Signaling	4.84
IL-9 Signaling	4.78
Semaphorin Neuronal Repulsive Signaling Pathway	4.77
Sperm Motility	4.75
Neuregulin Signaling	4.74
STAT3 Pathway	4.69
Granulocyte Adhesion and Diapedesis	4.68
HIF1 α Signaling	4.67
Germ Cell-Sertoli Cell Junction Signaling	4.67
PDGF Signaling	4.64
Cardiac Hypertrophy Signaling	4.60
IL-6 Signaling	4.60
G α i Signaling	4.52
Hepatic Fibrosis / Hepatic Stellate Cell Activation	4.46
Glioma Invasiveness Signaling	4.45
Agranulocyte Adhesion and Diapedesis	4.42
Regulation of the Epithelial-Mesenchymal Transition Pathway	4.42
Phagosome Formation	4.41
Erythropoietin Signaling Pathway	4.39
PTEN Signaling	4.36
Role of Tissue Factor in Cancer	4.30
Type II Diabetes Mellitus Signaling	4.27
Molecular Mechanisms of Cancer	4.26
Adrenomedullin signaling pathway	4.25
Glioblastoma Multiforme Signaling	4.24
IL-4 Signaling	4.23
Th1 and Th2 Activation Pathway	4.19

Table S6. Pathway analysis of gradient normoxia vs. hypoxia. Top 50 significant pathways ($p < 0.05$) identified from DEGs using Ingenuity Pathway Analysis.

Pathway	-log(p-value)
EIF2 Signaling	16.8
Huntington's Disease Signaling	14.1
Mitochondrial Dysfunction	12.5
Inhibition of ARE-Mediated mRNA Degradation Pathway	12.5
Regulation of eIF4 and p70S6K Signaling	10.9
Protein Ubiquitination Pathway	9.64
Oxidative Phosphorylation	9.53
Estrogen Receptor Signaling	9.16
PD-1, PD-L1 cancer immunotherapy pathway	8.93
FAT10 Signaling Pathway	8.92
Sirtuin Signaling Pathway	8.81
Glucocorticoid Receptor Signaling	7.94
BAG2 Signaling Pathway	7.51
mTOR Signaling	6.77
Th1 Pathway	6.23
Coronavirus Pathogenesis Pathway	5.37
Th1 and Th2 Activation Pathway	5.12
Antigen Presentation Pathway	5.10
Molecular Mechanisms of Cancer	4.81
Amyloid Processing	4.73
Th2 Pathway	4.53
PTEN Signaling	4.49
Insulin Receptor Signaling	4.34
Natural Killer Cell Signaling	4.29
Opioid Signaling Pathway	4.22
ID1 Signaling Pathway	4.19
Androgen Signaling	4.11
PEDF Signaling	4.08
α -Adrenergic Signaling	4.03
Leukocyte Extravasation Signaling	3.97
HER-2 Signaling in Breast Cancer	3.85
Fcy Receptor-mediated Phagocytosis in Macrophages and Monocytes	3.83
HGF Signaling	3.67
Neuroinflammation Signaling Pathway	3.66
Nucleotide Excision Repair Pathway	3.64
GP6 Signaling Pathway	3.60
Apelin Endothelial Signaling Pathway	3.52
CCR3 Signaling in Eosinophils	3.50
Mouse Embryonic Stem Cell Pluripotency	3.47
Apelin Cardiomyocyte Signaling Pathway	3.47
UVB-Induced MAPK Signaling	3.45
Sperm Motility	3.42
Thrombin Signaling	3.39
Nitric Oxide Signaling in the Cardiovascular System	3.38
Cardiac Hypertrophy Signaling (Enhanced)	3.30
Ketogenesis	3.30
Endocannabinoid Developing Neuron Pathway	3.22
CD40 Signaling	3.20
Apelin Adipocyte Signaling Pathway	3.18
EGF Signaling	3.17

Table S7. Pathway analysis of PC1 after comparative analysis with in vivo MI data. Top 50 significant pathways ($p < 0.05$) identified from PC gene loadings used as rankings in IPA.

Pathway	-log(p-value)
Colorectal Cancer Metastasis Signaling	3.99
P2Y Purigenic Receptor Signaling Pathway	3.05
CCR3 Signaling in Eosinophils	3.00
CDP-diacylglycerol Biosynthesis I	2.93
IL-1 Signaling	2.88
Phosphatidylglycerol Biosynthesis II (Non-plastidic)	2.83
Endocannabinoid Cancer Inhibition Pathway	2.81
Relaxin Signaling	2.71
Bladder Cancer Signaling	2.54
Hypoxia Signaling in the Cardiovascular System	2.45
Renin-Angiotensin Signaling	2.43
G α s Signaling	2.38
Endocannabinoid Developing Neuron Pathway	2.35
AMPK Signaling	2.33
Molecular Mechanisms of Cancer	2.33
SNARE Signaling Pathway	2.23
ID1 Signaling Pathway	2.15
MYC Mediated Apoptosis Signaling	2.07
IL-8 Signaling	2.06
RAN Signaling	2.05
Triacylglycerol Biosynthesis	2.04
Melanocyte Development and Pigmentation Signaling	2.02
Autophagy	2.01
Phototransduction Pathway	1.97
CSDE1 Signaling Pathway	1.93
Thrombin Signaling	1.92
α -Adrenergic Signaling	1.88
CXCR4 Signaling	1.84
Amyotrophic Lateral Sclerosis Signaling	1.77
Tumor Microenvironment Pathway	1.76
NGF Signaling	1.73
p38 MAPK Signaling	1.73
Endothelin-1 Signaling	1.67
Estrogen Receptor Signaling	1.66
GNRH Signaling	1.63
IL-7 Signaling Pathway	1.63
fMLP Signaling in Neutrophils	1.60
Biotin-carboxyl Carrier Protein Assembly	1.60
Leptin Signaling in Obesity	1.59
Role of MAPK Signaling in Inhibiting the Pathogenesis of Influenza	1.59
Adrenomedullin signaling pathway	1.58
Angiotensin Signaling	1.57
Antiproliferative Role of Somatostatin Receptor 2	1.57
Axonal Guidance Signaling	1.55
Insulin Secretion Signaling Pathway	1.55
HIF1 α Signaling	1.52
G α i Signaling	1.51
Opioid Signaling Pathway	1.50
Apelin Endothelial Signaling Pathway	1.50
Oxytocin Signaling Pathway	1.49

Table S8. Pathway analysis of PC2 after comparative analysis with in vivo MI data. Top 50 significant pathways ($p < 0.05$) identified from PC gene loadings used as rankings in IPA.

Data S1. (Separate file) Gene lists from differential expression analysis of the myocardial infarct border-zone-on-a-chip devices. The six pairwise comparisons include the gene name, p-value, FDR step up, and fold change.

Data S2. (Separate file) PC loadings. The principal component loadings for the first 18 components.

Data S3. (Separate file) Lists of upregulated and downregulated genes with similar expression profiles in the in vitro gradient and in vivo infarction but not in the uniform hypoxia condition. Gene lists include p-value and fold change.